

Autocorrelation spectra of an air-fluidized granular system measured by NMR

S. LASIČ¹, J. STEPIŠNIK^{1,2}, A. MOHORIČ¹, I. SERŠA² and G. PLANINŠIČ¹

¹ *University of Ljubljana, Faculty of Mathematics and Physics, Physics Department
Jadranska 19, 1000 Ljubljana, Slovenia*

² *Josef Stefan Institute - Jamova 39, 1000 Ljubljana, Slovenia*

received 9 February 2006; accepted in final form 18 July 2006

published online 11 August 2006

PACS. 45.70.Mg – Granular flow: mixing, segregation and stratification.

PACS. 76.60.Lz – Spin echoes.

Abstract. – A novel insight into the dynamics of a fluidized granular system is given by a nuclear magnetic resonance method that yields the spin-echo attenuation proportional to the spectrum of the grain positional fluctuation. Measurements of the air-fluidized oil-filled spheres and mustard seeds at different degrees of fluidization and grain volume fractions provide the velocity autocorrelation that differs from the commonly anticipated exponential Enskog decay. An empiric formula, which corresponds to the model of grain caging at collisions with adjacent beads, fits well to the experimental data. Its parameters are the characteristic collision time, the free path between collisions and the cage-breaking rate or the diffusion-like constant, which decreases with increasing grain volume fraction. Mean-squared displacements calculated from the correlation spectrum clearly show transitions from ballistic, through sub-diffusion and into diffusion regimes of grain motion.

Introduction. – Sand dunes, grain silos, building materials, catalytic beds, filtration towers, riverbeds, snowfields, and many foods are granular systems consisting of a large number of randomly arranged macroscopic grains. Despite their apparent simplicity, granular materials exhibit a host of unusual behaviors, whose unraveling more often than not appears to challenge the existing wisdom of science [1, 2].

A fluidized granular bed is a system of randomly arranged, macroscopic grains in which the driving force of motion is the shaking of a container or gas flow through the granular system. Although, these systems are of tremendous technological importance in the catalysis of gas-phase reactions, transport of powders, combustion of ores, and several other industrial processes, we do not have sufficient understanding of the fluid state of a granular medium that is analogous to macroscopic properties of liquids. Two particularly important aspects contribute to the unique properties of granular materials: thermodynamics plays no role, and interactions between the grains are dissipative, because of static friction and inelasticity of collisions. Several theoretical efforts start towards building granular fluid mechanics by considering the medium as a dense, inelastic gas with the temperature defined by induced local velocity fluctuations [3, 4]. The autocorrelation function of a single-particle velocity

fluctuation is the basis of many thermodynamic and hydrodynamic models that aim to provide a statistical description in terms of a single-particle dynamic [5, 6].

Although the experimental techniques used to study the motion of granular systems span a wide range of approaches and sophistication, attempts to grasp the details of grain motion in the fluidized state meet restraints of the applied instrumentation. Grain collisions are too fast for tracking by high-speed photography [7], by positron emission [8] or by CCD camera [9], while diffusing-wave spectroscopy discerns only the displacements shorter than the light wavelength [10]. Neither of them enables examination in the whole range of grain dynamics. Here we demonstrate a novel application of the NMR gradient spin-echo method, which can sample the spectrum of the bead positional fluctuation in an air-fluidized granular system in the entire range of motion from the fast grain-grain collisions to a slow diffusion-like motion. Generally, NMR is a tool that yields not only macroscopic properties as self-diffusion constant and flow velocity, but provides also information about single-particle dynamics due to the relation between the spin-echo attenuation and the motion on the micro-level [11, 12]. This potential of NMR can be exploited by the method of modulated gradient spin echo (MGSE), which was used for the analysis of molecular motion in porous media and emulsions [13–17] as well as for the interpretation of the pulsed gradient spin-echo (PGSE) measurements of granular motion [18, 19]. With the MGSE method, the periodic modulation of the spin phase yields the spin-echo attenuation proportional to the VA spectrum at the modulation frequency. The frequency range of reported MGSE applications was between a few Hz to about 1 kHz.

Herein, we present a novel application of the known MGSE technique with the extended frequency range to about 10 kHz, which is enough to scan the entire dynamic range of positional fluctuations in a fluidized granular system. In the case of weak enough gradients the Gaussian phase approximation can be used in the spin-echo analysis [20]. It gives the spin-echo attenuation [21]

$$\beta(\tau) = \frac{\gamma^2}{2\pi} \int_{-\infty}^{\infty} G(\omega, \tau) I_z(\omega) G^*(\omega, \tau) d\omega, \quad (1)$$

where the Fourier transform of the displacement autocorrelation function is the displacement power spectrum $I_z(\omega)$ [22]. It is equal to

$$I_z(\omega) = \frac{1}{\pi} \int_{-\infty}^{\infty} \langle \Delta z(t) \Delta z(0) \rangle e^{-i\omega t} dt, \quad (2)$$

where $\Delta z(t) = z(t) - \langle z(t) \rangle$ is the component of the particle displacement fluctuation around the mean trajectory of motion in the direction of the applied magnetic-field gradient. Knowledge of $I_z(\omega)$ gives the VA spectrum, $D(\omega) = I_z(\omega) \omega^2$, and also the time-dependent mean-squared displacement $\langle [z(t) - z(0)]^2 \rangle = \frac{4}{\pi} \int_0^\infty I_z(\omega) (1 - \cos(\omega t)) d\omega$.

The effect of MGSE sequence can be described by an effective gradient, whose spectrum $G(\omega, \tau) = \int_0^\tau G_{eff}(t) e^{-i\omega t} dt$ defines the relation between the spin echo and the spin displacement in eq. (1). The gradient spectrum of the most commonly used PGSE sequence [23–25] has the zero-frequency lobe that prevents the discrimination of fast collisional motions from slow air-driven ones [26]. The four-gradient-pulse variant of PGSE, applied to remove the effect of flow motion of fluidized grains [18], has a too broad gradient spectrum to sample $I_z(\omega)$ [12]. However, the spectrum of its multi-pulse variant, the MGSE sequence, has a single narrow peak that can be used to sample $I_z(\omega)$ [26].

Although the Carr-Purcell-Meiboom-Gill sequence with the train of π -RF pulses (CPMG) [27] is available with the most commercial NMR set-up, also as a tool to remove the effect of motion, a novel approach to the analysis of its spin-echo attenuation displays it as

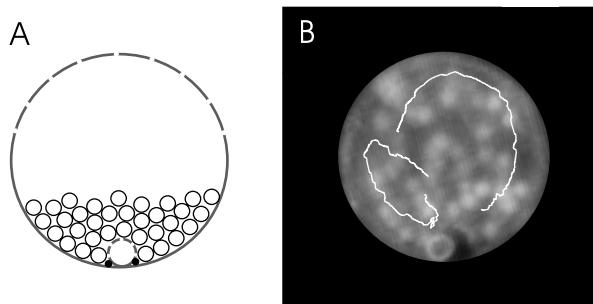


Fig. 1 – A) The schematic drawing of the experimental cell side view with the system at rest, where grains are packed around the perforated hose. B) Snapshot of the air-fluidized system through the side window by the high-speed camera. The curves show the trajectories of two representative grains during 80 ms long interval that is about four times longer than the duration of the applied MGSE sequence.

an efficient MGSE sequence for the motional analysis of spin-bearing particles [28,29], when applied together with a constant magnetic-field gradient. The sequence of RF pulses superimposed to the magnetic-field gradient excites multiple spin coherence pathways [30], which accumulate the spin dephasing and the resulting motional attenuation in different manners [31,32]. By isolating the direct coherence pathway, the frequency range of the novel MGSE sequence depends only on the repetition rate of applied π -RF pulses and not on the switching of gradient pulses that are created by the induction-limited currents in the surrounding coil system. Its gradient spectrum has the dominant peaks at $\omega_m \pm \frac{2\pi}{T}$, if π -RF pulses are repeated at $T/2$ intervals. By changing T , the variation of the spin-echo attenuation at $\tau = NT$,

$$\beta(\tau, \omega_m) = \frac{8\gamma^2 G^2 \tau}{\pi^2} I_z(\omega_m), \quad (3)$$

enables the measurement of the spectrum $I_z(\omega)$. Thus, the MGSE method provides the ensemble average distribution of the particle displacement fluctuation with respect to the frequency of motion, in which the hydrodynamic flow field appears at very low frequencies, usually outside of the dynamic range of the method.

Experimental procedure. – The experiment was carried out on a TecMag NMR spectrometer with a 2.35 T horizontal bore superconductive magnet that was equipped with micro-imaging accessories and Maxwell gradient coils.

The novel MGSE technique, with $16 \mu\text{s}$ long π -RF pulses of the CPMG train, was applied to measure the motion in the air-fluidized dilute granular gas of the pharmaceutical 3 mm diameter, oil-filled, hard-plastic spherical beads with restitution coefficient 0.85 and of the mustard seeds of 2 mm averaged diameter and restitution coefficient 0.55. The system bed was the cylindrical chamber built from a piece of a plastic syringe tube of 26 mm length and 23.5 mm diameter that was placed inside the RF coil with the cylinder axis aligned horizontally. The perforated hose of 5 mm outer diameter, attached to the bottom inner wall, played the role of a diffuser for the air up-flow that lifted beads into the motion. Several holes of 0.5 mm diameter, drilled uniformly across the wall of the container, served as air outlets (fig. 1A). The pressure of air, introduced through the perforated hose, regulated the degree of fluidization. The grain volume fraction of fluidized pharmaceutical beads was about 0.18, while the mustard seeds were measured at different grain contents.

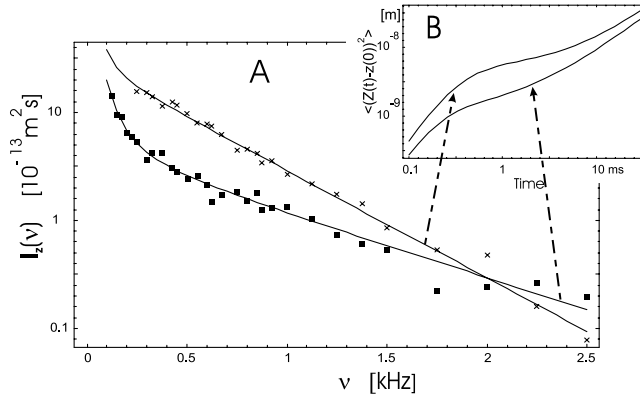


Fig. 2 – A) The displacement fluctuation spectra of oil-filled beads fluidized by air flow at a pressure of 0.25 bar (squares) and of 0.5 bar (crosses) show a clear exponential decrease at higher frequencies. B) The Fourier transforms of the curves, which represent the best fit of an empiric formula to the data, give the mean-squared displacements of grains that clearly show three regimes of motion: ballistic, sub-diffusion and diffusion.

A static gradient field of 0.0625 T/m was applied in the horizontal direction, perpendicular to the axis of the cylindrical container, and perpendicular to the static magnetic field. The average amplitude of eight co-added spin-echo signals was recorded at different modulation periods, T , but at constant acquisition time $t = NT = 20$ ms, which determines the low-frequency limit of the measurement. The duty cycle of our RF amplifier limits the highest modulation frequency of the MGSE measurement to about 10 kHz.

Results and discussion. – The high-speed video recording at framing rates of 600 fps makes it possible to inspect visually the grain motion occurring in the proximity of transparent container walls. The grain trajectories obtained from successive snapshots were superimposed to a single snapshot in fig. 1B. The traces represent the motion of two grains during 50 movie steps corresponding to the time interval about four times longer than the duration of the applied MGSE sequence. Trajectories do not represent a time-averaged hydrodynamic flow field but locations of a bead taken by consecutive camera frames. A thorough examination of the movie revealed a tendency of grains to move in clusters, which are continually forming and dispersing within the fluidized system. A grain mainly follows the cluster motion, but small zigzag deviations of its trajectory, hardly seen in fig. 1B, indicate the existence of fast grain-grain collisions inside a moving cluster-cage. There was no noticeable evidence of air bubbles. The snapshots permit to estimate the position variation of the time-average bead volume fraction in the fluidized state. An average over 1000 frames shows a variation of about $\pm 15\%$ across the container horizontal diameter and decreases for about 50% going from the bottom to the top of the container. As during the time of MGSE sequence, the mean length of the grain trajectory is only about one-third of the container diameter, the effect of grain collisions with the walls is negligible compared to the effect of grain-grain collisions, which are a bit faster than the speed of our camera, but are in the frequency range of the novel MGSE technique. MGSE measurements of oil-filled spheres at different gas pressures give the spectra $I_z(\omega)$ that exhibit a clear exponential decrease at frequencies above 400 Hz as shown in fig. 2. The fast grain motion at air pressure of 0.5 bar amplifies the high-frequency part, while it hinders the examination at low frequencies due to the strong signal attenuation. The reduction of air

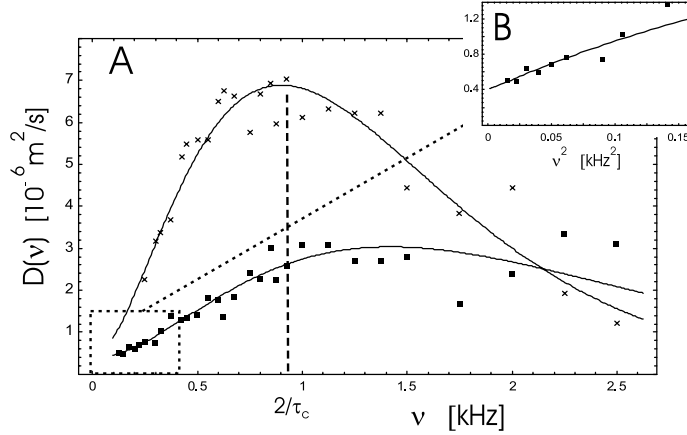


Fig. 3 – A) The velocity autocorrelation spectrum of grains in the system of oil-filled beads fluidized by the air flow at 0.25 bar (squares) and at 0.5 bar (crosses). B) The intersection $D(0)$ gives the cage-breaking rate, while the line slope is related to the mean path of beads between collisions.

pressure to 0.25 bar slows down the motion enough to observe the part of spectrum below 400 Hz, which passes from the exponential to $1/\omega^2$ -dependence. Figure 3A shows the VA spectrum, $D(\omega) = I_z(\omega)\omega^2$, that does not display the Lorentzian form as expected for the Enskog VA spectrum. The positron emission measurement of the VA spectrum in the vibro-fluidized granular bed gave a similar spectral lobe but with a poor resolution above 1 kHz [8]. Authors attributed the observed lobe to the grain collisions with the walls of the experimental cell. However, the frequency ranges of the novel MGSE technique, which can go beyond 3 kHz, can provide better insight into the fast grain motion as follows.

The low-frequency part of $D(\omega)$ in fig. 3B exhibits a ω^2 -dependence, which resembles the VA spectrum of a restricted diffusion in porous media. There, the low-frequency slope of $D(\omega)$ vs. ω^2 plot is related to the mean size of pores, while the intersection $D(0)$ is equal to the inter-pore long-time diffusion rate [33]. Along this line, the measured $D(\omega)$ of fluidized granular systems can be treated with the model, in which the adjacent colliding beads close the grain into a cage that breaks apart after a few collisions [4]. Thus, the low-frequency slope of $D(\omega)$ vs. ω^2 can be related to the length of the mean path of the grain between collisions, while $D(0)$ could describe the cage-breaking rate, which we consider as a sort of diffusion constant. The measurement of the air-fluidized system of mustard seeds in the same experimental set-up gives $D(0)$, which decreases with increasing bead volume fraction as shown in fig. 4. It seems that a higher grain density leads to the formation of larger clusters that slow down the cage-breaking rate. The observation with the snapshots of high-speed photography confirms this assumption. The exponential decrease of $I_z(\omega)$, fig. 2 at high frequencies is very different from the Lorentzian form typical for the restricted diffusion in porous media. By taking into account the measured exponential dependence of spectra at high frequencies and the low-frequency dependence as in the restricted diffusion case, which is also supported by the taken snapshots of the constrained grain motion in the clusters, we propose an empiric formula,

$$I_z(\omega) = \frac{D + \langle \xi^2 \rangle \tau_c \omega^2}{\omega^2} e^{-\tau_c \omega}. \quad (4)$$

The fitting parameter $\sqrt{\langle \xi^2 \rangle}$ is attributed to the mean-squared free path of the bead, τ_c to the mean collision interval and D to the diffusion-like cage-breaking rate. Interestingly,

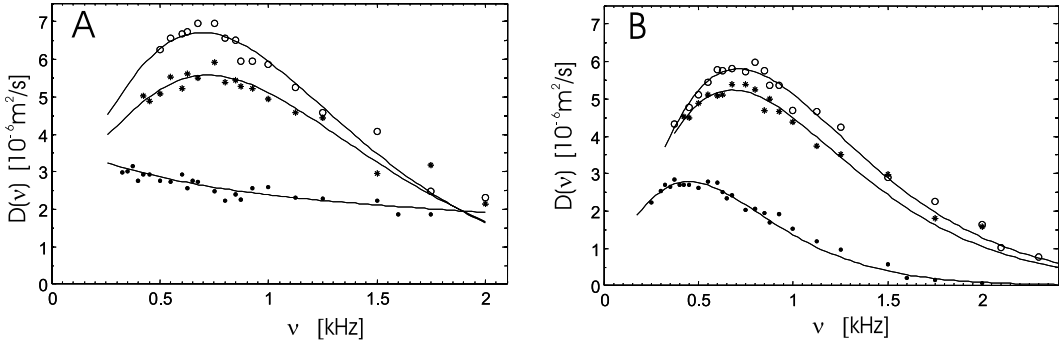


Fig. 4 – The power spectrum of the grain velocity fluctuation in the system of mustard seeds fluidized by the air flow at 0.25 bar (dots) and 0.5 bar (stars) and 1 bar (circles) at two different fillings: A) 150 seeds and B) 175 seeds. The fitting parameters of the curves (from bottom to top) are: A) $\langle \xi^2 \rangle = 0.22, 3.6, 4.8 \times 10^{-9} \text{ m}^2$, $\tau_c = 0.11, 0.39, 0.42 \text{ ms}$, $D = 3.8, 3.8, 3.6 \times 10^{-6} \text{ m}^2/\text{s}$ and B) $\langle \xi^2 \rangle = 3.1, 4.2, 4.65 \times 10^{-9} \text{ m}^2$, $\tau_c = 0.65, 0.45, 0.44 \text{ ms}$, $D = 1.4, 1.3, 0.6 \times 10^{-6} \text{ m}^2/\text{s}$.

the time dependence of the mean-squared displacement, calculated from $I_z(\omega)$ in fig. 2B, gives the time dependence that was already observed by the optical measurement and by the imaging [34, 35]. In the short-time ballistic regime, it goes as t^2 , in the intermediate sub-diffusion regime as t^α with $\alpha < 1$, and in the long-time diffusion regime as t .

The best fit of the formula to the experimental data gives the curves shown in figs. 2 and 3. For the air flow at 0.25 bar, the fitting parameters are: $\langle \xi^2 \rangle = 1.2 \times 10^{-9} \text{ m}^2$, $\tau_c = 0.22 \text{ ms}$ and $D = 0.47 \times 10^{-6} \text{ m}^2/\text{s}$, with the error of 5%. The air flow at 0.5 bar gives a very clear exponential dependence on the fitting parameters: $\langle \xi^2 \rangle = 4.4 \times 10^{-9} \text{ m}^2$, and $\tau_c = 0.36 \text{ ms}$, but less exact $D = 0.6 \times 10^{-6} \text{ m}^2/\text{s}$ due to the attenuation cut-off at the low frequencies. From this formula, the $D(\omega)$ -maximum is at $2/\tau_c$. The results indicate that the grain motion generates surprisingly rapid collisions at displacements much smaller than the grain diameter. Such fast and small displacements, which have not been perceived either by positron emission measurements or by imaging methods, were indeed observed by the diffusing-wave spectroscopy on differently fluidized granular systems [10, 34].

The Fourier transform of $D(\omega)$ gives the grain VA function with the mean square of velocity fluctuation $\langle \Delta v_z(0)^2 \rangle$, which is considered as a measure of the temperature in the fluidized system. Thus, the Fourier transforms of the fitting curves in fig. 3 give an increase of the system temperature for a factor 1.3 as the pressure increases from 0.25 bar to 0.5 bar. Analysis of MGSE measurements on the air-fluidized system of mustard seeds with the enlarged content of grains reveals an increase of the collisional partition in the VA spectrum and the decrease of the cage-breaking rate $D(0)$ at higher grain density.

Conclusions. – The broad frequency range of the novel variant of a NMR modulated gradient spin method makes it possible to scan the grain motion in the air-fluidized granular systems from fast ballistic collisions to slow diffusion-like motion. The measured VA function differs from the anticipated Enskog exponential decay and points out to a highly correlated process with a slow diffusion superposed to rapid collisions at lengths much smaller than the grain diameter. Measurements display the reduction of cage-breaking rate with the increase of grain density.

* * *

We are grateful to the Slovenian Ministry for High Education, Science and Technology for financial support. We thank E. FUKUSHIMA, New Mexico Resonance Group, who provided some grains for our measurements.

REFERENCES

- [1] JAEGER H. M. and NAGEL S. R., *Rev. Mod. Phys.*, **68** (1996) 1259.
- [2] DE GENNES P. G., *Physica A*, **261** (1998) 267.
- [3] BAGNOLD R. A., *Proc. R. Soc. London, Ser. A*, **225** (1954) 49.
- [4] JENKINS J. T. and SAVAGE S. B., *J. Fluid Mech.*, **130** (1983) 187.
- [5] ENSKOG D., *Arch. Mat. Astron. Fys.*, **16** (1922) 16.
- [6] ALDER B. J. and WAINWRIGHT T. E., *Phys. Rev. Lett.*, **18** (1967) 988.
- [7] WILDMAN R. D., HUNTLEY J. M. and HANSEN J. P., *Phys. Rev. E*, **60** (1999) 7066.
- [8] WILDMAN R. D., HANSEN J. P. and PARKER D. J., *Phys. Fluids*, **14** (2002) 232.
- [9] UTTER B. and BEHRINGER R. P., *Phys. Rev. E*, **69** (2004) 031308.
- [10] DURIAN D. J., *J. Phys.: Condens. Matter*, **12** (2000) A507.
- [11] DE GENNES P. G., *Phys. Lett. A*, **29** (1969) 20.
- [12] STEPIŠNIK J., *Physica B*, **104** (1981) 350.
- [13] CALLAGHAN P. T. and STEPIŠNIK J., *J. Magn. Reson. A*, **117** (1995) 118.
- [14] STEPIŠNIK J. and CALLAGHAN P. T., *Physica B*, **292** (2000) 296.
- [15] CALLAGHAN P. T. and CODD S. L., *Phys. Fluids*, **13** (2001) 421.
- [16] TOPGAARD D., MALMBORG C. and SOEDERMAN O., *J. Magn. Reson.*, **156** (2002) 195.
- [17] PARSONS E. C., DOES M. D. and GORE J. C., *Magn. Reson. Imaging*, **21** (2003) 279.
- [18] SEYMOUR J. D., CAPRIHAN A., ALTABELLI S. A. and FUKUSHIMA E., *Phys. Rev. Lett.*, **84** (2000) 266.
- [19] CAPRIHAN A. and SEYMOUR J. D., *J. Magn. Reson.*, **144** (2000) 96.
- [20] STEPIŠNIK J., *Physica B*, **270** (1999) 110.
- [21] STEPIŠNIK J., *Europhys. Lett.*, **60** (2002) 453.
- [22] KUBO R., TODA M. and HASHITSUME N., *Statistical Physics II: Nonequilibrium Statistical Mechanics* (Springer-Verlag) 1991.
- [23] CANDELA D., DING A. and YANG XIAOYU, *Physica B*, **279** (2000) 120.
- [24] SAVELSBERG R., DEMCO D. E., BLUEMICH B. and STAPF S., *Phys. Rev. E*, **65** (2002) 020301(R).
- [25] MAIR R. W., CORY D. G., PELED S., TSENG CHING HUA, PATZ S. and WALSWORTH R. L., *J. Magn. Reson.*, **135** (1998) 478.
- [26] CALLAGHAN P. T. and STEPIŠNIK J., *Advances in Magnetic and Optical Resonance*, edited by WARREN S. WARREN, Vol. **19** (Academic Press, Inc, San Diego) 1996, Chapt. *Generalised Analysis of Motion Using Magnetic Field Gradients*, pp. 326-389.
- [27] MEIBOOM S. and GILL D., *Rev. Sci. Instrum.*, **29** (1958) 688.
- [28] STEPIŠNIK J., LASIČ S., MOHORIČ A., SERŠA I. and SEPE A., to be published in *J. Magn. Reson.* (2006).
- [29] LASIČ S., STEPIŠNIK J. and MOHORIČ A., to be published in *J. Magn. Reson.* (2006).
- [30] HURLIMANN M. D., *J. Magn. Reson.*, **148** (2001) 367.
- [31] ZIELINSKI L. J. and SEN P. N., *J. Magn. Reson.*, **164** (2003) 145.
- [32] ZIELINSKI L. J. and SEN P. N., *J. Chem. Phys.*, **119** (2003) 1093.
- [33] STEPIŠNIK J., MOHORIČ A. and DUH A., *Physica B*, **307** (2001) 158.
- [34] MENON N. and DURIAN D. J., *Science*, **275** (1997) 1920.
- [35] MARTY G. and DAUCHOT O., *Phys. Rev. Lett.*, **94** (2005) 015701.